

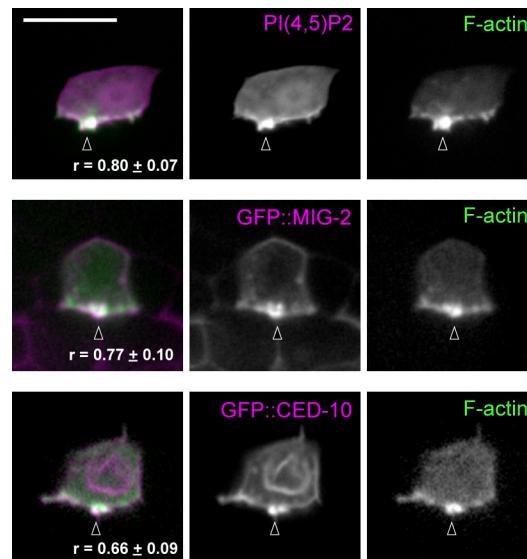
Hagedorn et al., <http://www.jcb.org/cgi/content/full/jcb.201312098/DC1>

Figure S1. **F-actin and invadopodial membrane components are tightly colocalized in wild-type animals.** Lateral view images show ACs coexpressing the F-actin marker *cdh-3* > mCherry::moeABD (green in overlays, left) with the invadopodial membrane components PI(4,5)P2 (visualized with GFP::PLC δ^{PH}), GFP::MIG-2, and GFP::CED-10 (magenta in overlays). F-actin and all invadopodial membrane components localized tightly together within invadopodia at the invasive cell membrane (arrowheads). Pearson's correlation coefficients (r) for colocalization are shown as mean \pm SEM ($n \geq 5$ animals each genotype).

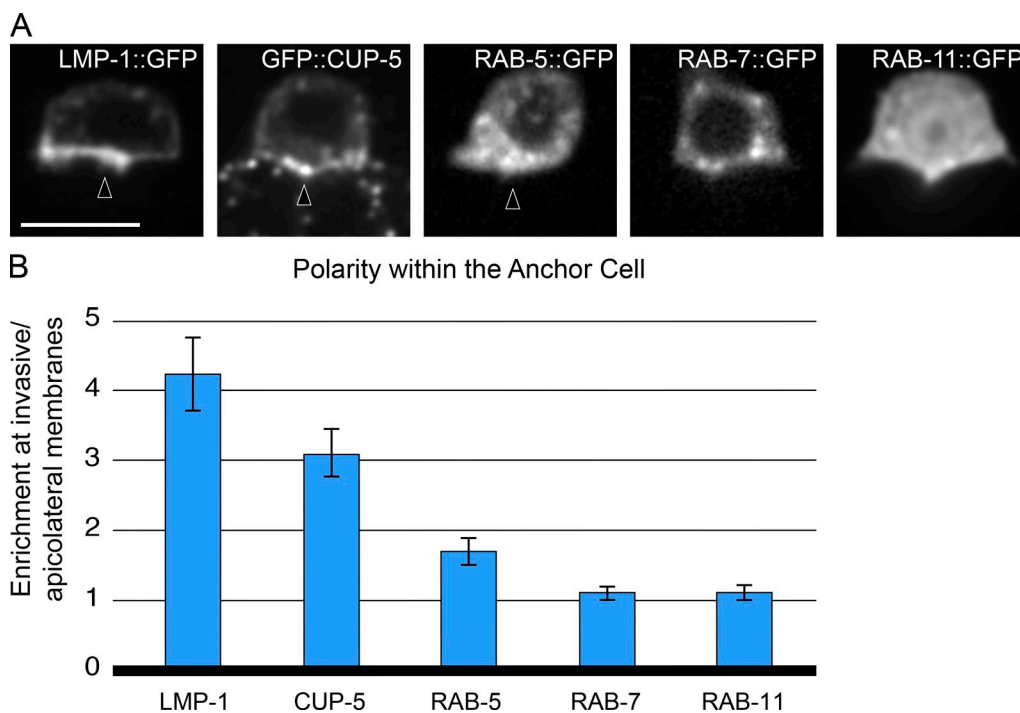


Figure S2. **Polarization of lysosomal but not endosomal proteins during AC invasion.** (A) Early (Rab5; mCherry::RAB-5), late (Rab7; mCherry::RAB-7), and recycling (Rab11; mCherry::RAB-11) endosomal proteins do not enrich at the invasive membrane during AC invasion. However, the lysosomal proteins LMP-1 (mCherry::LMP-1) and CUP-5 (GFP::CUP-5) are highly polarized (three- to fourfold) to the invasive membrane. Lateral-view images; bars, 5 μ m. (B) Graphs report the fold enrichment of the endosomal and lysosomal markers at the invasive membrane ($n \geq 5$ animals examined for each genotype, error bars report \pm SEM).

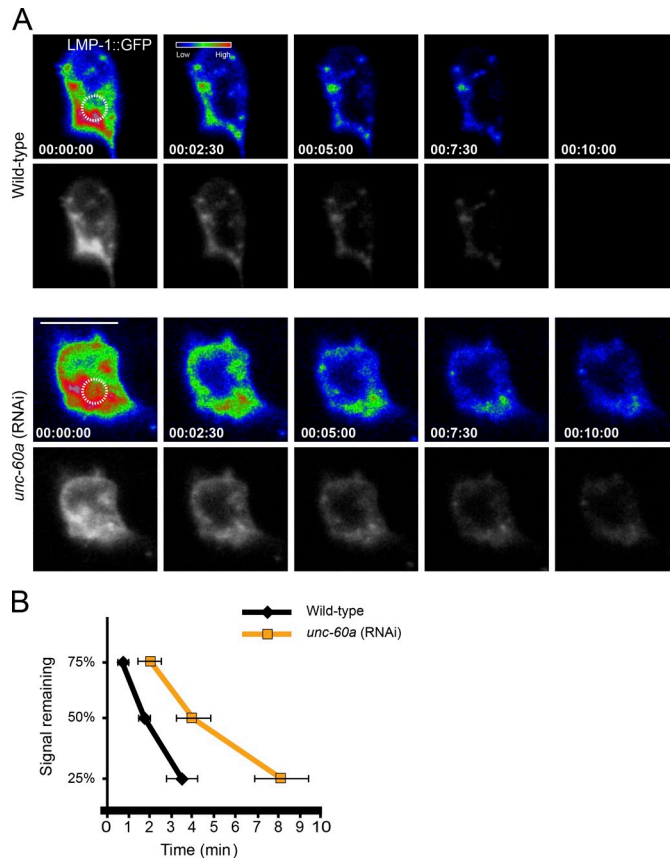
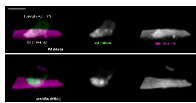
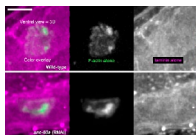


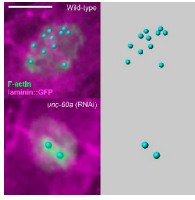
Figure S3. **Invadopodial membrane recycling from the endolysosome is regulated by UNC-60A.** (A) Focused laser photobleaching of an $\sim 1.0\text{-}\mu\text{m}$ region above the invasive membrane (circle) in a wild-type AC (top row) resulted in over 50% loss of the endolysosome LMP-1::GFP signal throughout the AC within 2.5 min (time-points, minutes). The LMP-1::GFP signal persisted for longer in *unc-60a* (RNAi) animals. The original fluorescent images are shown underneath images depicting a heat map of the fluorescent intensity. (B) Graphs report LMP-1::GFP signal remaining at the nonbleached invasive membrane over time ($n \geq 5$ animals each genotype; $P < 0.05$ for 25, 50, and 75% signaling remaining; Student's t test).



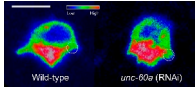
Video 1. **UNC-60A (ADF/cofilin) regulates F-actin dynamics during invadopodia formation.** Lateral-view time-lapses show 3D reconstruction of F-actin in wild-type (top) and *unc-60a* RNAi-treated (bottom) ACs. F-actin is visualized with *cdh-3 > mCherry::moeABD* (green); the basement membrane is visualized with *laminin::GFP* (magenta). Images were acquired using a spinning-disk confocal microscope (CSU-10 scan head; Yokogawa Corporation of America) mounted on an upright microscope (AxioImager; Carl Zeiss). 43-min time-lapses are shown with time-points acquired every 60 s. Projections of seven z-sections (step size of $1\ \mu\text{m}$) are shown. The video plays at 10 frames per second. Bar, $5\ \mu\text{m}$. This video corresponds to Fig. 2 C.



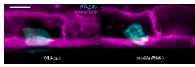
Video 2. **UNC-60A (ADF/cofilin) regulates F-actin dynamics during invadopodia formation.** Ventral-view time-lapses show 3D reconstruction of F-actin in wild-type (top) and *unc-60a* RNAi-treated (bottom) ACs. F-actin is visualized with *cdh-3 > mCherry::moeABD* (green); the basement membrane is visualized with *laminin::GFP* (magenta). Images were acquired using a spinning-disk confocal microscope (CSU-10 scan head; Yokogawa Corporation of America) mounted on an upright microscope (AxioImager; Carl Zeiss). 60-min time-lapses are shown with time-points acquired every 15 s. Projections of eight z-sections (step size of $0.5\ \mu\text{m}$) are shown. The video plays at 10 frames per second. Bar, $5\ \mu\text{m}$. This video corresponds to Fig. 2 C.



Video 3. **Spot-tracking analysis of AC invadopodia lifetimes.** Ventral-view time-lapses show a wild-type (top) and *unc-60a* RNAi-treated animal (bottom) just before the normal time of basement membrane breaching in wild-type animals. F-actin (*mCherry::moeABD*) is shown in green and laminin (*laminin::GFP*) is shown in magenta; spots (cyan) are overlaid on fluorescence (left) and shown alone (right). Time points were acquired every 15 s and the video plays at a rate of 10 frames per second. Bar, 5 μ m. This video corresponds to Fig. 2 D.



Video 4. **FLIP analysis reveals dynamic recycling of invadopodial membrane through the endolysosomal compartment.** Lateral-view time-lapses show spectral representation of fluorescence intensity of LMP-1::GFP in wild-type (left) and *unc-60a* RNAi-treated (right) ACs. Small 1- μ m regions of the invasive membrane (circles) were continuously photobleached using 100% laser power and 20 iterations. The first time-point shown is immediately before the start of photobleaching. This analysis was performed using a confocal microscope (LSM 510; Carl Zeiss) equipped with a 100x objective. 10-min time-lapses are shown with time-points acquired every 30 s. The video plays at 10 frames per second. Bar, 5 μ m. This video corresponds to Fig. 5 A.



Video 5. **The invadopodial membrane component PI(4,5)P₂ localizes to static intracellular membrane vesicles in the absence of *unc-60a* (ADF/cofilin).** Lateral-view time-lapses show 3D reconstruction of PI(4,5)P₂ in wild-type (left) and *unc-60a* RNAi-treated (right) ACs. PI(4,5)P₂ is visualized with *cdh-3 > mCherry::PLC δ ^{PH}* (cyan); the basement membrane is visualized with *laminin::GFP* (magenta). Images were acquired using a spinning-disc confocal microscope (CSU-10 scan head; Yokogawa Corporation of America) mounted on an upright microscope (AxioImager; Carl Zeiss). 40-min time-lapses are shown with time points acquired every 60 s. Projections of seven z-sections (step size of 1 μ m) are shown. The video plays at 10 frames per second. Bar, 5 μ m. This video corresponds to Fig. 5 B.

Table S1. **Extrachromosomal array and integrated stain generation**

| Strain designation ^a | PCR fusion created | Injected concentration | Co-injection marker |
|---------------------------------|-----------------------------------|------------------------|---------------------|
| qyEx237 | <i>unc-60 > GFP::unc-60a</i> | 0.1 ng/ μ l | unc-119+ |
| qyEx236, qyls224 | <i>cdh-3 > GFP::Cbrunc-60</i> | 0.1 ng/ μ l | unc-119+ |
| qyEx235, qyls222, qyls223 | <i>cdh-3 > GFP::unc-60a</i> | 0.1 ng/ μ l | unc-119+ |
| qyEx282 | <i>cdh-3 > Dendra2::act-1</i> | 0.1 ng/ μ l | unc-119+ |
| qyEx411 | <i>zmp-1 > Imp-1::mCherry</i> | 0.1 ng/ μ l | unc-119+ |
| qyEx403 | <i>cdh-3 > GFP::cup-5</i> | 0.1 ng/ μ l | unc-119+ |
| qyls211 | <i>cdh-3 > Imp-1::GFP</i> | 0.1 ng/ μ l | unc-119+ |
| qyls205 | <i>cdh-3 > mCherry::rab-11</i> | 0.1 ng/ μ l | unc-119+ |
| qyls252 | <i>cdh-3 > mCherry::rab-7</i> | 0.1 ng/ μ l | unc-119+ |
| qyls256 | <i>cdh-3 > mCherry::rab-5</i> | 0.1 ng/ μ l | unc-119+ |

^aEx signifies an extrachromosomal transgenic line, whereas *ls* denotes stably integrated lines.

Table S2. Primer sequences and templates used for PCR fusions

| Primer sequence | Primer type | Amplicon | Template |
|--|--------------------------------------|--------------------------|---------------------------|
| 5'-TAATGTGAGTGTAGCTCACTCATTAGG-3' | Forward | <i>cdh-3</i> > promoter | pPD107.94/mk62-63 |
| 5'-AACGATGGATACGCTAACCACTTGG-3' | Forward, nested | <i>cdh-3</i> > promoter | pPD107.94/mk62-63 |
| 5'-TTTCTGAGCTCGGTACCTCCAAG-3' | Reverse | <i>cdh-3</i> > promoter | pPD107.94/mk62-63 |
| 5'-AGTATTGCCAGAAAATCCCGTTGC-3' | Forward | <i>unc-60</i> > promoter | Fosmid WRM0613bD01 |
| 5'-CTCTTAATGTGAGCCTAGTGCTCG-3' | Forward, nested | <i>unc-60</i> > promoter | Fosmid WRM0613bD01 |
| 5'-TCACGTGTGAGATCACAGTTGCCG-3' | Forward, nested 2 | <i>unc-60</i> > promoter | Fosmid WRM0613bD01 |
| 5'-GAAAAGTCTTCTCCTTTACTCATACTCTA GAAAACAGGCACACATAG-3' | <i>gfp</i> extension, reverse | <i>unc-60</i> > promoter | Fosmid WRM0613bD01 |
| 5'-ATGAGTAAAGGAGAAGAACTTTTC-3' | Forward | <i>GFP</i> | pPD95_81 |
| 5'-TTTGTATAGTTCATCCATGCCATG-3' | Reverse | <i>GFP</i> | pPD95_81 |
| 5'-CATGGCATGGATGAACATACAAATCCGGT GTCATGGTCGACCCAGAT-3' | <i>gfp</i> extension, forward | <i>unc-60a</i> | Fosmid WRM0613bD01 |
| 5'-TCATGGTCGTGGAATTACACGGCC-3' | Reverse | <i>unc-60a</i> | Fosmid WRM0613bD01 |
| 5'-TTAGGCTTAGGCTGGGCTTAGCC-3' | Reverse, nested | <i>unc-60a</i> | Fosmid WRM0613bD01 |
| 5'-ATAGGCTCAAGCTTAGGCTTAGGC-3' | Reverse, nested 2 | <i>unc-60a</i> | Fosmid WRM0613bD01 |
| 5'-ATTACACATGGCATGGATGAACAAATGGTGACT GACTAGTTTTTGGCT-3' | <i>gfp</i> extension, forward | <i>Cbrunc-60</i> | AF16 genomic DNA |
| 5'-AGGATCCGAACATGGTCAAAACGG-3' | Reverse | <i>Cbrunc-60</i> | AF16 genomic DNA |
| 5'-AATATGTGGGATTGCTTTAAAACG-3' | Reverse, nested | <i>Cbrunc-60</i> | AF16 genomic DNA |
| 5'-ATGTGTGACGACGAGGTTGC-3' | Forward | <i>act-1</i> | <i>C. elegans</i> genomic |
| 5'-ACTTCCCTTCTGTTCAAAG-3' | Reverse | <i>act-1</i> | <i>C. elegans</i> genomic |
| 5'-CGGAAGTTATCATAACAACCG-3' | Reverse, nested | <i>act-1</i> | <i>C. elegans</i> genomic |
| 5'-ATGAACCTTATTAAGGAAGA-3' | Forward | <i>Dendra2</i> | <i>Dendra2</i> plasmid |
| 5'-CCATGCTTGACTTGGTAGAG-3' | Reverse | <i>Dendra2</i> | <i>Dendra2</i> plasmid |
| 5'-AAGGGCCCTTCGCCATTTACATCGGCTC-3' | Forward | <i>cup-5</i> | pHD736 |
| 5'-AAGAGCTCGTACGGCCGACTAGTAGG-3' | Reverse | <i>cup-5</i> | pHD736 |
| 5'-AATTAATTAAGACGCTGGCATATCCTTGT-3' | Reverse | <i>lmp-1</i> | <i>C. elegans</i> genomic |
| 5'-AAACCGGTATGTTGAAATCGTTTGTATC-3' | Forward | <i>lmp-1</i> | <i>C. elegans</i> genomic |
| 5'-AAAAGCGGTTAGCTCCTTCGGTCC-3' | Reverse | <i>rab-5</i> | pHD281 |
| 5'-TCTGTGACTGGTGAGTACTCAACC-3' | Reverse, nested | <i>rab-5</i> | pHD281 |
| 5'-AAAAGCGGTTAGCTCCTTCGGTCC-3' | Reverse | <i>rab-7</i> | pHD251 |
| 5'-TCTGTGACTGGTGAGTACTCAACC-3' | Reverse, nested | <i>rab-7</i> | pHD251 |
| 5'-CTTGGAGGTACCGAGCTCAGAAAATGGTCTCAA GGTGAAGA-3' | <i>cdh-3</i> , extension, forward | <i>rab-11</i> | pJWZ529 |
| 5'-CAGGAAACAGCTATGACCATG-3' | Reverse | <i>rab-11</i> | pJWZ529 |
| 5'-CATTACAGGACAAAGAGAGGG-3' | Reverse, nested | <i>rab-11</i> | pJWZ529 |